Jurnal Kejuruteraan SI 4(1) 2021: 19-32
https://doi.org/10.17576/jkukm-2021-si4(1)-03

Experimental Study for Determining the Diameter of Plasma Channel and Energy Distribution Ratio into Workpiece during WEDM Process of AISI 316

(Kajian eksperimental untuk menentukan diameter saluran plasma dan nisbah pengagihan tenaga ke dalam benda kerja semasa proses WEDM AISI 316)

Adel S.O. Warregh[a,*] & Zahiruddin M. Md. Zain[a]

[a] *School of manufacturing, University Malaysia Perlis, Kampus Tetop U/u Pauh, Jalan Arau- Changlun 02600 Arau, Perlis, Malaysia*

**Corresponding author: adelsaleh201313@yahoo.com*

Received 4 March 2021, Received in revised form 19 April 2021
Accepted 30 August 2021, Available online 30 September 2021

ABSTRACT

Electrodes removal phenomena of WEDM is important to understand the efficiency and the process accuracy. To clarify and understand the phenomenon, the plasma channel diameter and distribution of energy into electrodes are required. However, reports on the distribution of energy and plasma channel diameter are scarce. In this work, the energy distribution and plasma diameter of WEDM process were obtained. By comparing the melted material boundary in the crater obtained by the metallographic approach with the curve isothermal of the thermo-physical model obtained by finite element modelling (FEM), the distribution of energy besides that diameter of the plasma channel of the WEDM process were estimated. From this study, results indicate that the expansion of the diameter of the plasma channel must be taken into consideration in order to be more consistent with the real WEDM process. By applying the proposed method in this study, the distribution of energy and diameter of plasma channel, in various dielectrics with different polarities were investigated. However, by comparing the findings of the current study with the previous works, it turns out that the distribution of energy into the workpiece and the diameter of the plasma channel may be calculated by this approach.

Keywords: Energy distribution; Wire electrical discharge machining (WEDM); diameter of plasma channel; crater; Finite element modelling (FEM)

ABSTRAK

Fenomena penyingkiran elektrod WEDM adalah penting bagi memahami kecekapan dan ketepatan proses. Untuk menjelaskan dan memahami fenomena tersebut, diameter saluran plasma dan pengagihan tenaga adalah diperlukan ke dalam elektrod. Walau bagaimanapun, laporan mengenai pengagihan tenaga dan diameter saluran plasma adalah jarang. Dalam karya ini, pengagihan tenaga dan diameter plasma proses WEDM telah diperolehi. Dengan membandingkan batas bahan cair di kawah yang diperoleh melalui pendekatan metallografi dengan lengkung isotermal model termo-fizikal yang diperoleh melalui pemodelan elemen hingga (FEM), pengagihan tenaga dan diameter saluran plasma proses WEDM telah dianggarkan. Daripada kajian ini, hasil menunjukkan bahawa pengembangan diameter saluran plasma mesti diambil kira agar lebih konsisten dengan proses WEDM yang sebenar. Dengan menerapkan kaedah yang dicadangkan dalam kajian ini, penyebaran tenaga dan diameter saluran plasma, dalam pelbagai dielektrik dengan polariti yang berbeza telah diselidiki. Namun, dengan membandingkan hasil kajian semasa dengan kajian sebelum ini, ternyata pengagihan tenaga ke dalam benda kerja dan diameter saluran plasma dapat dikira melalui pendekatan ini.

Kata kunci: Pengagihan tenaga; Mesin pelepasan elektrik wayar (WEDM); Diameter saluran plasma; Kaedah elemen hingga (FEM); kawah

INTRODUCTION

In industrial applications, electrical discharge machining (EDM) is widely used. This non-contact approach will machine any electrically conductive or semi-conductive material regardless of hardness (Abu Qudeiri et al. 2019; Bilal et al. 2019). Since the advent of EDM technology, it has been roughly 70 years. However, the research topics are also focused on improving the method by looking at fundamental physical phenomena. In general, EDM process is a mechanism of thermal eroded that involves heat transfer. Some generalized thermo-mathematical models based on heat conduction equations have been proposed to simulate the thermal mechanism (Hou et al. 2014; Joshi & Pande 2010b; Kumar et al. 2015; Liu & Guo 2016; Shahri et al. 2017). In other words, an EDM is a process of material removal that uses electrical discharge energy as the major source of energy. The total electrical discharge energy is transmitted into the anode (workpiece) and cathode (tool electrode) during the EDM process, and it is lost into the gap (distance between the electrodes). The energy that is distributed into electrodes is converted to heat, and some of it erodes the workpiece and the tool electrode. This fact explains why the distribution of energy into electrodes is the most important factor in determining the EDM process's efficiency and accuracy. Accordingly, the distribution of energy into electrodes (cathode and anode) can be considered as a significant factor, to clarify the EDM process performance. This paper suggested a method for determining and calculating the ratio of energy distribution and diameter of plasma channel by the comparison between the molten material boundary within the crater which was gained by the metallographic approach and surface isothermal for thermo-physical model gained by applying finite element modelling (FEM). In a manner analogy to conventional method (Allen & Chen 2007a; Hayakawa et al. 2001; H. Singh 2012; H. Singh & Shukla 2012; Xia, H., Kunieda, M. & Nishiwaki 1996; Zahiruddin & Kunieda 2010), in the begining, the boundary of the molten material which re-solidified within discharge crater were determined using metallographic approach; then the molten material boundary was calculated by the thermo-physical model by using finite element modelling by assume the ratio of energy distribution into anode (workpiece). Besides that the diameter of plasma channel (i.e., diameter of q0). The calculation will be repeated even the simulated and measured boundaries coincides. In addition, the findings of the ratio of energy distribution during EDM anode and cathode (electrodes) can be used for further research works regarding the fundamental of sinking EDM process like; determination of the arc plasma radius, investigation of the energy consumption during process of removal, and understanding the workpiece deformation as result thermal stresses which were generated by temperature changes.

LITERATURE REVIEW

Electrodes removal phenomena of WEDM are important to understand the performance of the process. Distribution of total discharge energy into electrodes is an important subject to explain the phenomena. However, nowadays only few researchers worldwide reported on energy distribution in case of sinking EDM. According to a review of the literature, several researchers have estimated the rate of material removal (Allen & Chen 2007a; Gostimirovic et al. 2018; Joshi & Pande 2010a) (workpiece erosion per unit time), and thermal residual stress (Gostimirovic et al. 2018; Shabgard, Seydi & Seyedzavvar 2016; Zahiruddin & Kunieda 2016). Thickness of the recast layer and surface roughness (Warregh & Zain 2018) on the basis of thermo-mathematical models. Within the discharge area, the supplied energy was converted to thermal energy and was essentially distributed between the anode (workpiece), cathode (tool electrode), and dielectric fluid. A variety of physical process consumed the energy, including; sparking, explosion, melting, vaporization, conduction, and radiation. The amount of distribution of energy within workpiece previously was thought it is a significant determinant for WEDM efficiency (Rajendran & Vendan 2015; Shao & Rajurkar 2015). The diameter of the plasma channel, in addition to the energy distribution, was an important and critical consideration. According to (Zahiruddin & Kunieda 2012), the power density, which is determined by the discharge energy and plasma channel diameter, may have a significant effect on the energy and removal efficiencies for WEDM. As a result, precise determination of the ratio of energy distribution into the workpiece and plasma channel diameter will provide critical and insightful information for better understanding the basic physical mechanism of the WEDM process and increasing its implementation potential and ability. The energy distribution has been calculated since 1975 by (Xue et al. 2012). By measuring the temperatures of both tool electrode, workpiece, and dielectric fluid. (Xia, Kunieda & Nishiwaki 1996; Hayakawa et al. 2001) measured the distribution of energy by comparing the measured temperatures of electrodes with simulated findings getted under the supposed ratio of distribution of energy into both cathode and anode (electrodes). At the beginning, the rise of temperature within the cathode (Cu tool electrode) was measured by using a thermocouple; after that, the rise of temperature into the cathode (tool electrode) was also calculated by the thermal conduction model by supposing the ratio of energy distribution into the cathode (- ve). The

calculation will be repeated until the measured temperature coincides with the simulated temperature, and the supposing ratio was thought to be the ratio of energy that got lost into the Cu tool electrode due to conduction as a percentage of overall discharge energy. This approach has also been used in several recent studies (H. Singh 2012; H. Singh & Shukla 2012; Zahiruddin & Kunieda 2010, 2012). This approach was used by (Singh 2012; Singh & Shukla 2012) to investigate the ratio of energy distribution in electrodes of tungsten-carbide. The ratio of the energy distribution into micro EDM electrodes was studied by (Zahiruddin & Kunieda 2010, 2012). In general, the thermocouple was typically placed and fixed at a near distance from the discharge point, and the temperature rises signal was observed milliseconds after discharge. In order to prevent electromagnetic noise, the observed positioning of the thermocouple, the geometry of the electrodes, and the equipment's ability to withstand electromagnetic noise all played a role in measurement precision. As a result, detecting the energy distributed through the electrode with this procedure is extremely difficult. Since the discharging occurred in such a significantly small space and continue for such a short period (short time), the precise measuring radius of the plasma channel was extremely difficult. (Escobar, de Lange & Castillo 2020) used a video camera with high-speed to determine the arc plasma radius. However, a photographed light-emitting zone does not appear to be the plasma arc region where discharge current flows, and the photographed radius is dependent on camera settings like time of exposure and aperture of diaphragm. As a result, the video camera with high-speed cannot accurately determine the radius of arc plasma. (Kojima, Natsu & Kunieda 2008), who determined the radius of the plasma channel using spectroscopic techniques. They found that after a dielectric breakup, the arc plasma expands entirely in a few microseconds, while the diameter of craters grow steadily in addition to the arc plasma's expanding speed. Their exploration differs from traditional plasma expansion models that are focused on the observation of generated craters.

ENERGY DISTRIBUTION MODEL OF WEDM

The total discharge energy generated between the workpiece and tool electrode is dispersed into them and lost within their gap, as illustrated in Figure 1a. The energy distributed into electrodes is then consumed for material removal and taken away by debris, lost by heat conduction inside electrodes, and lost due to heat convection and radiation, as seen in Figure 1b. (Hayakawa et al. 2001) calculated the heat flux due to convection and radiation at the long discharge duration and found that it is negligibly small, with the majority of the discharge energy being conducted through the anode (workpiece) and cathode (tool electrode). Energy losses due to heat convection and radiation can be neglected, and the energy distribution into both cathode (tool electrode) and anode (workpiece) is only controlled by the energy loss due to heat conduction inside electrodes and the energy transmitted away by debris. As a result, the ratio of energy distribution into electrodes is determined in this study based on the addition of the loss of energy ratio as a result of heat conduction to the energy ratio transferred away by debris.

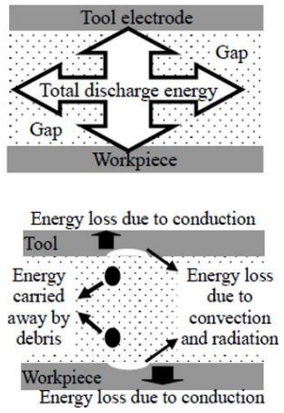

FIGURE 1. Distribution of energy into WEDM electrodes (Zahiruddin & Kunieda, 2010)

PRINCIPLE

The metal (material) was extracted (removed) from both cathode and the anode during WEDM machining. Only the workpiece will be investigated for simplification in current work. Figure 2 demonstrates the distribution of energy through the workpiece. X is the proportion of energy transmitted through the workpiece to overall discharge energy. A minor portion of X was lost due to debris, while the remainder was lost due to heat conduction (Hayakawa et al. 2001; Zahiruddin & Kunieda 2010). Figure 2 demonstrates the ratios of energy carried away by debris and energy wasted due to heat conduction within the workpiece as X_{deb} and X_{con}, respectively, in relation to the overall discharge energy:

$$X = X_{con} + X_{deb} \tag{1}$$

By using a metallographic technique, the volume of debris (V) was determined experimentally, and ratio of energy taken away by debris (X_{deb}) was calculated based on the thermal property of the experiment material and debris volume (V).

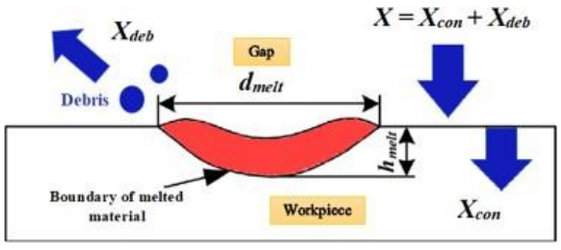

FIGURE 2. Discharge energy distributed into workpiece

$$X_{deb}=(E_{debm}+E_{debv})/i_e.u_e.t_e \quad (2)$$

$$V=V_m+V_v \quad (3)$$

When the material is removed by melting and vaporization, E_{debm} and E_{debv} are the amounts of energy taken away by debris. The volume of debris removed by melting and vaporization is V_m and V_v, respectively. The discharge current, discharge voltage, and discharge duration are described by i_e, u_e, and t_e, respectively. Since the breakdown delay was so brief in our experiments, the discharge time was referred to as pulse duration in the following.

$$E_{debm}=\rho_{Vm}[c(T_{mv}-T_s)+L_m] \quad (4)$$

$$E_{debv}=\rho V_v[c(T_v-T_s)+L_m+L_v] \quad (5)$$

Where: ρ is the density [kg/m^3], c is the specific heat [J/(kg K)], T_{mv} is the temperature between melting and boiling point, T_v is the boiling point, T_s is the average temperature of the workpiece before the single discharge, Lm is the heat of fusion [J/kg], L_v is the evaporation heat [J/kg].

The efficiency of removal, R_e,or η was defined as the debris volume ratio, V, regarding to the total melted volume, V_s.

$$R_e=\frac{V}{V_s} \quad (6)$$

DETERMINATION OF ENERGY DISTRIBUTION INTO WORKPIECE

Figure 3 shows a flowchart which indicates a method to determine energy distribution ratio into workpiece. As explained in the previous section, energy distributed into the workpiece was swept away by debris and lost due to conduction. The energy taken away by debris is calculated in this paper using the method proposed by (Zahiruddin & Kunieda 2012) by supposing the ratio of removal by vaporization to total removal volume as follow:

$$g=\frac{V_v}{V} \quad (7)$$

g = 0 indicates that all of the debris was removed by melting, while g = 1 indicates that all of the debris was removed by vaporization. X_{con}'s worth was unknown. In principle, at the begining, the unknown X_{con} is supposed to be between 0 and 1 and then multiplied by the total discharge energy obtained from the waveform recorded by the oscilloscope equipment in order to calculate the energy conducted into the workpiece. Another required parameter for the calculation of the power density on the workpiece surface is the plasma radius, R_{pc}. The R_{pc} value was considered to be between 50 μm (0.05 mm) and R_{max} similar to the case of X_{con}. According to the findings reported by (Kojima, Natsu & Kunieda 2008), the value of R_{max} was set to 500 m (0.5 mm). The step size for X_{con} and R_{pc} was set to 0.1 % and 5 μm, respectively, during the calculation. The values of X_{con} and R_{pc} were determined by comparing the measured and simulated boundaries of the melted material, as seen in Figure 3. The crater's whole geometry parameters were compared, including melted material diameter (d_{melt}), melted material depth (h_{melt}), and melted material volume (V_s). When the difference between observed and simulated values of all three parameters is less than 3%, it is considered a coincidence. Only the crater diameter was compared in an analysis by Zahiruddin & Kunieda (2012). In general, a controlling equation was the well-known Fourier heat conduction equation.

$$\frac{\delta^2 T}{\delta r^2}+\frac{1}{r}\frac{\delta T}{\delta R}+\frac{\delta^2 T}{\delta Z^2}=\frac{1}{\alpha}\frac{\delta T}{\delta t} \quad (8)$$

Where: r is the radial axis (m), Z is the vertical axis (m), t is time (s), T is the temperature (K), and α is the material's thermal diffusivity (m^2/s) which can be written as:

$$\alpha=\frac{K_t}{\rho C_P} \quad (9)$$

Where: ρ denotes the material density (kg/m^3), K_t denotes the material's thermal conductivity (J/m K s) and C_P denotes the specific heat (J/kg K).

The melting heat was taken into account in current work by re-modifying the thermal diffusivity contained in the Fourier equation for heat conduction.

$$\alpha^t=\frac{K_t}{\rho\left(C_p+L_m/T_m\right)} \quad (10)$$

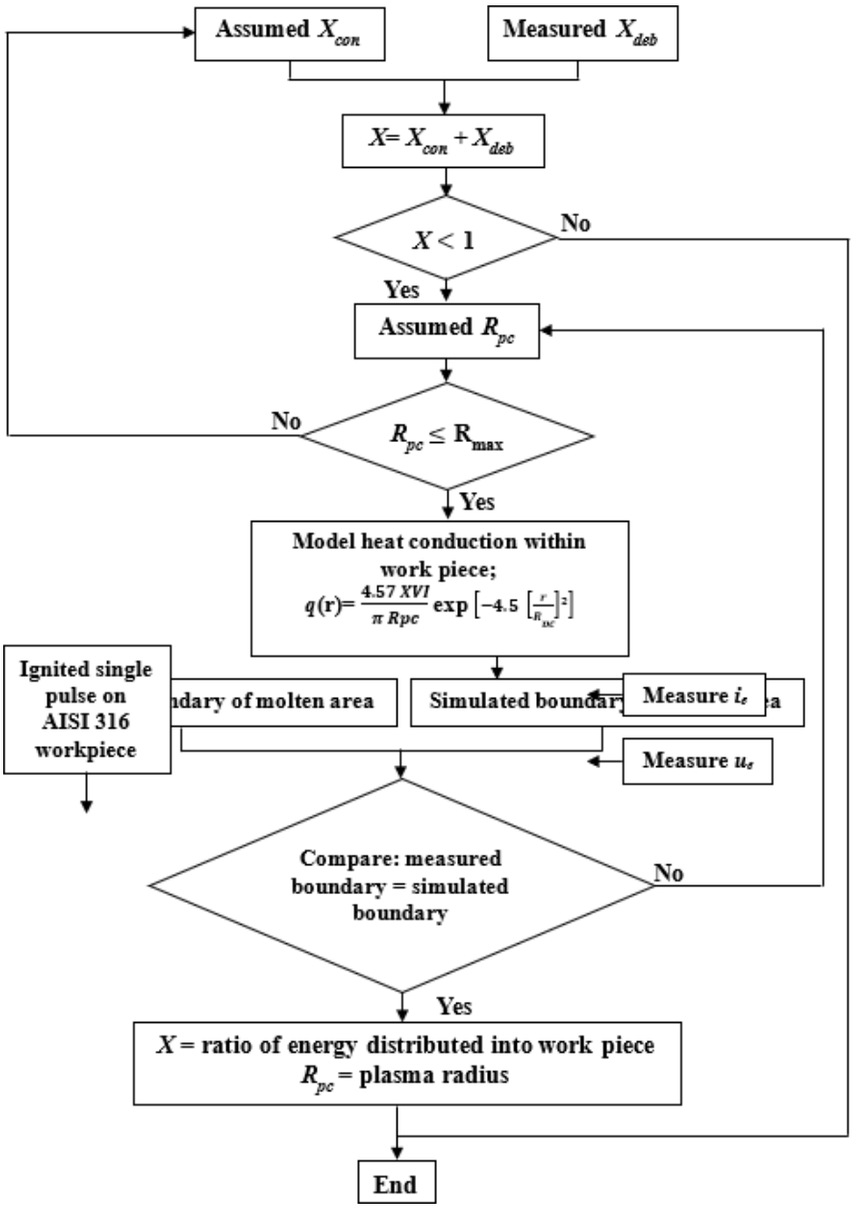

FIGURE 3. Method for determination of energy distribution into workpiece

DIAMETER OF PLASMA

It is worth noting that the plasma diameter is still controversial to this day because of the inability to correctly test it. Different researchers have made various empirical calculations to predicting the diameter of the plasma (Izquierdo et al. 2009; Kitamura & Kunieda 2014; Revaz, Witz & Flükiger 2005; Xue et al. 2012). However, there is a significant difference between the empirical equations proposed by different researchers. At the begining, the radius of the plasma during the discharge is considered to be constant in present work based on the findings of (Kojima, Natsu & Kunieda 2008), who stated that arc plasma finishes expanding within a few microseconds after dielectric breakdown. The calculation was then re-modified based on the calculation results of the value of Rpc for various pulse discharges, taking into account the variance of the plasma radius during the discharge, and they have stated that the plasma expands five times the crater size.

HEAT SOURCE

Aside from the plasma diameter, the kind of heat source is another critical aspect that can have a major impact on the simulation findings. Even where the discharge energy and

plasma diameter are the same, the simulated findings vary greatly depending on the heat source (Shao & Rajurkar 2015). In the case of WEDM, plane, circular, point, and gauss heat sources were commonly used in the region of heat conduction (Joshi & Pande 2010b; Shao & Rajurkar 2015; H. Singh 2012).The gauss heat source was the most widely used and usually considered to be more accurate in the actual case of certain types of heat sources (Joshi & Pande 2010b; M. Singh et al. 2020). The heat from the plasma was approximated using the Gauss distribution of heat flux in this study. The following equation describes the heat q that enters the workpiece as a result of an EDM spark:

$$q_0 = (4.57 X u_e i_e)/(\pi R^2_{pc}) \quad (11)$$

The maximum heat flux q_0 can be calculated as follow:

$$q(r) = q_0 \exp\left(-4.5 \left(\frac{r}{Rpc}\right)^2\right) \quad (12)$$

Where: X is portion from the total WEDM spark power directed at the workpiece.

EXPERIMENT

WORKPIECE MATERIAL

Stainless steel AISI 316 is selected as the workpiece material, with size was 50 mm × 14.2 mm × 3 mm as demonstrated in Figure 4.

FIGURE 4. Workpiece material used in experiment

EQUIPMENT

The equipment used in the setup of the experiment to measure the single pulse discharge is illustrated in Figure 5, and the equipment used for measuring the removal depth of the workpiece is illustrated in Figure 6.

TABLE 1. Parameters used for single pulse discharge experiment

Parameter & unit	Value	Reason for chosen of parameters values
The polarity of an anode (workpiece)	Positive and negative	The energy transmitted into the anode and cathode was different even for the same electrode material, according to the findings of an inquiry conducted by (Shen et al. 2014; Xia, H., Kunieda, M., & Nishiwaki 1996; Zhang et al. 2016). In this study, in order to research the influence of polarity on ratio of energy distribution in this case, positive and negative polarities were used, comparing our findings to previous findings.
Pulse on time (Ton; µs)	55,100,210, 290	A wide variety of pulse on time (pulse durations) were used to investigate the variation of distribution of energy with the pulse on time (pulse duration).
Distance of the Electrode (µm)	50,100,200, 400	According to research performed by (Kojima, Natsu, and Kunieda 2008), the electrode' distance had a significant impact on the diameter of the discharge plasma channel. As a consequence, this study looked into the influence of electrode' distance on the characteristic of energy distribution.
Electrode Shape	Needle and disk	In the current contexts, different electrode forms were used and the effect of the electrode shape had to be investigated.
Voltage (V)	45	That is the typical value of the discharge current and discharge voltage, respectively.
Current (A)	20	

MACHINING PARAMETERS USED

Table 1 demonstrates the values of the input parameters which used in the experiment.

EXPERIMENTAL SETUP

Figure 5 demonstrates the equipment for single pulse discharge. A ball screw was used to monitor the distance between both cathode (needle as electrode) and anode (workpiece) that was calibrated with a micrometer gauge. In each experiment, the breakdown delay period was controlled through five seconds by adjusting the gap between the cathode and the anode.

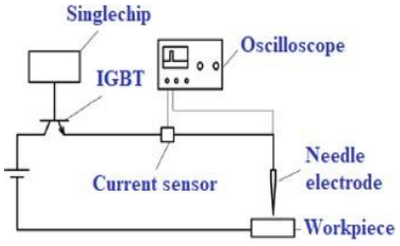

FIGURE 5. Single pulse discharge experimental setup

The difference between discharge time and pulse discharge can be overlooked because the time of the breakdown delay was significantly shorted. As a result, in this work, the debate was conducted using the expression "discharge of pulse." The shape of single pulse discharge waveform was generated by usage only a single chip (89C52RC) to controlling the make-and-break of an IGBT (SGL160N60UFD). By changing the program parameters of the single chip, it is simple to acquire the different pulse discharge. The peak voltage of the waveform was 45 V, and the average current during the discharge was about 20 A. The overall discharge energy was measured by analysing the voltage and current waveforms captured by an oscilloscope. Stainless steel 316 was used as the workpiece. While as tool electrode, a brass needle was used.

EXPERIMENT PROCEDURE

Following discharge of the single pulse, the sample was cut then embedded in epoxy. Nikon's most advanced metallurgical microscope (Nikon Eclipse MA200) was used to gain a section view of the crater after it had been polished and etched with nital. Then, after the etching process, it can be observed clearly the profile of recast region that was used to reconstruct the three-dimensional model of the crater. Around 15–20 segment photos were taken for each crater. Distance between each segment was almost 20–30 µm. The distance between each segment can be precisely measured using a micrometre gauge, as seen in Figure 6.

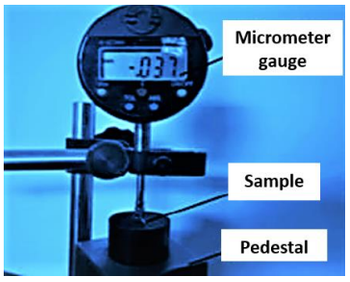

FIGURE 6. Equipment utilized for measurement of workpiece's removal depth

The crater's appearance were reconstructed using 3D-CAD tools (Solidworks). Figure 7 depicts the appearance of the re-solidified material in the craters. By using the three-dimensional model, the crater's entire structure, including the diameter of molten material, d_{melt}, depth of molten material, h_{melt}, the extracted material volume (debris), V, and volume of molten material, V_s, can be determined.

Experiments in various dielectrics (de-ionized water, kerosene, and air) with various machining polarities were carried out with a wide range of discharge durations(55–290 µs). Table 1 illustrates the parameters settings used in the experiment.

RESULTS AND DISCUSSION

Determination the energy lost ratio that carried away by debris, X_{deb}

As explained in the begining of this work, by debris volume and thermo- physical properties for material of workpiece, the X_{deb} was determined.

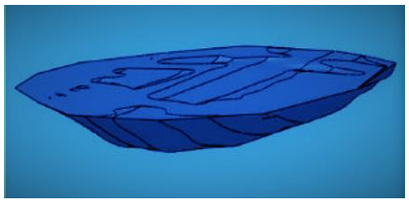

FIGURE 7. Three dimensional model of the resolidified material at crater

Figure 7 illustrates a 3D model of the craters, which was used to determine the volume of the debris. Figure 8 illustrates the values of X_{deb} and g (the ratio of removal by vaporisation to overall removal volume) in dielectric fluid (de-ionized water) with polarity (+ve). Except when the discharge duration was 55 µs, the X_{deb} values were significantly small, as seen in Figure 8. The higher efficiency of removal when the discharge duration was 55

μs may justify this. The efficiency of removal was 15.9% in this study's experiment when the discharge duration was 55 μs. This (15.9%) was considerably higher than the values stated by other authors (1–10%) (Van Dijck 1973). This may be attributed to the fact that the conditions of the experiments were different.

The efficiency of removal was significantly low with longer discharge durations (100–290 μs), as was X_{deb}. This means that the majority of the molten material was re-solidified within the crater rather than being removed, and that the energy amount taken away by debris was minimal. Effects of g (the removal ratio by vaporization to total volume of removal) would be negligible in this case. In the present experiments, the value of removal efficiency was positive when the pulse discharge was 210 and 290 μs. The variation of density of the re-solidified material as a result of the metallographic structure changing may be explaining this. According to a review of the literature (Hayakawa et al. 2001; Xia, Kunieda & Nishiwaki 1996; Zahiruddin & Kunieda 2012), in sinking EDM process, the energy carried away by debris is significantly small and can be ignored.

DETERMINATION THE ENERGY LOST RATIO BY CONDUCTION OF HEAT, X_{CON} AND RADIUS OF PLASMA CHANNEL, R_{PC}

At beginning, the molten material boundaries are determined using the metallographic approach, in order to make comparison between the measured boundaries and simulated boundaries. Figure 9 shows a cross section of the crater obtained in dielectric fluid (de-ionized water) with polarity (+ve), at various discharge durations, and Figure 10 illustrates the molten material boundaries obtained from the photographs.

SIMULATION BY SUPPOSING A CONSTANT PLASMA RADIUS, R_{PC} DURING DISCHARGING.

In current section, the simulation was carried out with supposing a constant plasma radius during the discharging, and the findings are illustrated in Figure 11. With discharge duration, the value of both X_{con} and R_{pc} increases, as seen in Figure 11. The R_{pc} values vary greatly depending on the various discharge durations. For example, when the discharge duration was 55 and 290 μs, the value of R_{pc} was 0.12 and 0.44 mm, respectively, indicating that supposing a constant value of R_{pc} did not coincide with the actual case.

By fitting the value of R_{pc} at various pulse discharges, it appears that the R_{pc} value can be fit by this equation:

$$R_{pc}=\mathrm{K}t_e^n \tag{13}$$

Where: K is a coefficient as well as n.

The outcome shows that during discharging, the radius of plasma channel did not remain stable. The following section took into account the shift in radius of the plasma channel over time in order to be more accurate. This conclusion is consistent with previous research. (Izquierdo et al. 2009; Revaz, Witz & Flükiger 2005), the expansion of the plasma radius was calculated using an equation similar to Eq (13).

SIMULATION BY SUPPOSING AN EXPANDS PLASMA RADIUS, R_{PC} DURING DISCHARGING

Figure 12 demonstrates how the variance of the heat flux, q, on the surface of the workpiece was calculated by the variation pattern of the radius of the plasma channel demonstrated in Figure 11.

The value of q is determined by R and t_e. Because of the small radius of plasma of discharge, the maximum value of q, i.e. q_0, is significantly high at an early stage of discharging, as seen in Figure 12. The increase in the discharge plasma radius causes a sudden decrease in the value of q_0. In addition, previous research (Izquierdo et al. 2009) verified this q_0 decrement. This means that during discharging, the heat flux (power density) would decrease. (Zahiruddin & Kunieda 2012) investigated the relationship between micro and sinking EDM removal efficiency and energy efficiency, which is described as the ratio of energy carried away by debris to energy transmitted into anode (workpiece), also they concluded that the power density was a crucial and significant factor influencing on both removal efficiency and energy efficiency.

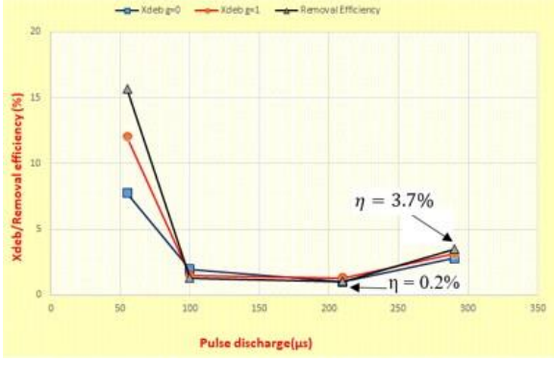

FIGURE 8. X_{deb} variation and efficiency of removal with discharge duration; machining conditions: in dielectric fluid (de-ionized water) with (+ve) polarity.

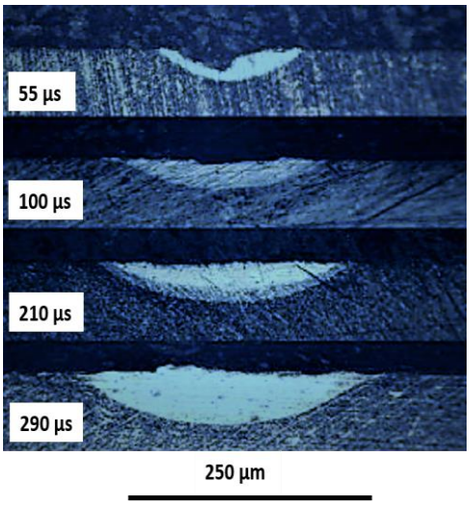

FIGURE 9. Molten material cross section within crater at various discharge durations.

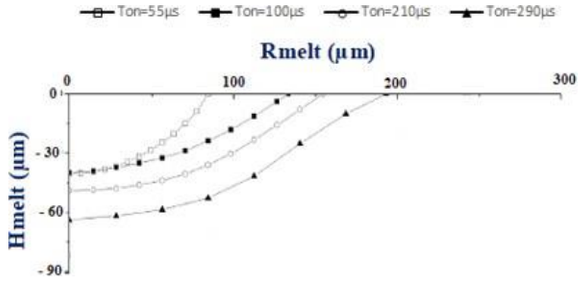

FIGURE 10. Boundaries of melted material

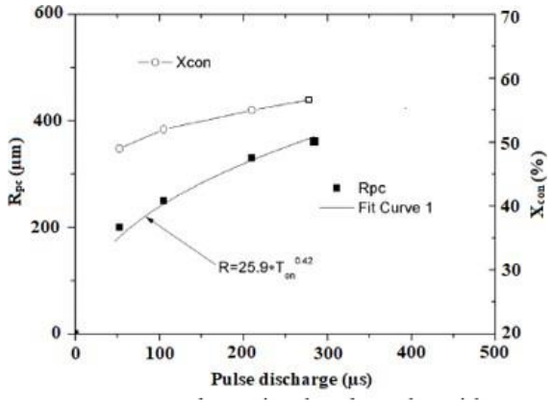

FIGURE 11. X_{con} and R_{pc} simulated results with constant radius of the plasma.

Since the expansion of the plasma radius was reduced in the case of micro EDM as a result of the relatively short pulse length, the heat flux (power density) was extremely high, about 30 times that of case sinking EDM (Zahiruddin & Kunieda 2012). According to the findings of (Zahiruddin & Kunieda 2012), variation of the radius of plasma channel during discharging has a major impact on the efficiency of both energy and removal. The higher removal efficiency at 55 µs in this work can be clarified by the higher heat flux (power density) at the beginning of the discharging, as seen in Figure 12.

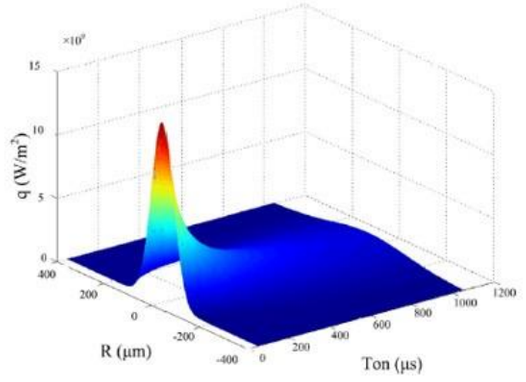

FIGURE 12. Heat flux variation and evolution with pulse discharge.

By employing Eq. (13) in this work, the expansion of the plasma radius was implemented. The R_{pc} value was changed in flowchart seen in Figure 3 by changing the n's value in Eq. (13). Figure 13 compares the values of X_{con} gained with a radius of an expanding plasma channel to those gained with a fixed plasma radius. Figure 14 shows the n's value and trend of expanding plasma radius for various discharge durations. X_{con} was much smaller in value than that obtained by consistent plasma radius when plasma radius was expanded. In Figure 14, the n's value was different, so maybe this can be interpreted that due to random experiments. Figure 15 illustrates the evolution of the boundary of molten material with different R_{pc}. With constant radius of plasma channel, extra energy was needed to melt the same material volume, as illustrated in Figure 15 (a). Furthermore, as the pulse discharge ranges from 55 to 290 µs, the boundaries that was simulated were not consistent with the boundaries that was measured which are illustrated in Figures 9 and 10. Figure 15 (b) illustrates the boundaries that was simulated of the molten material with expanding plasma radius, and the simulated and measured findings are very similar. In this work, the simulation results show that the plasma radius differed from the plasma radius reported by (Kojima, Natsu & Kunieda 2008). According to above analysis, it was concluded that by taking plasma expansion into account would be more consistence with the actual EDM.

INFLUENCE OF DIELECTRIC FLUID AND POLARITY ON DISTRIBUTION OF ENERGY AND PLASMA RADIUS

Influences of dielectric fluid and polarity on distribution of energy and radius of plasma channel were studied by the approach suggested in this paper.

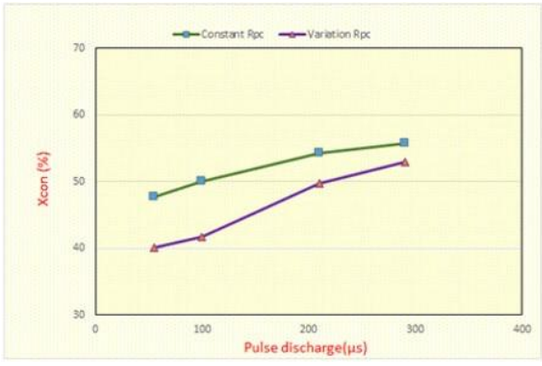

FIGURE 13. Values of X_{con} obtained with expanding Rpc compared with constant R_{pc} at various pulse discharge

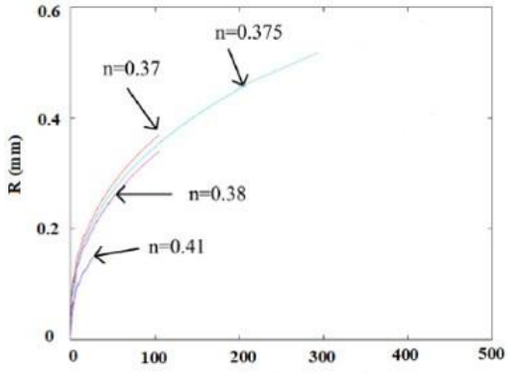

FIGURE 14. n's Value, and plasma radius expanding tendency at various discharge durations.

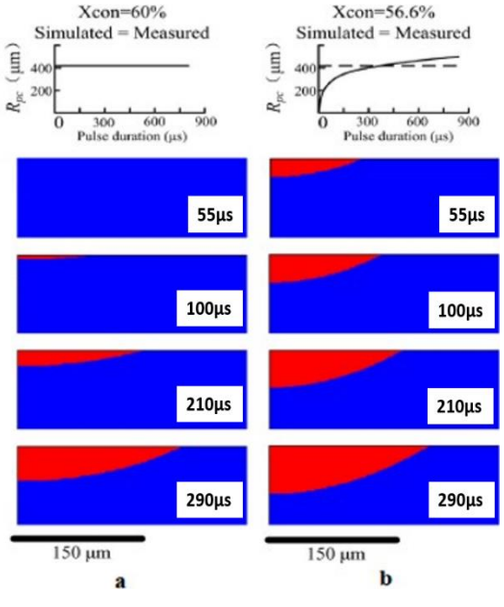

FIGURE 15. Simulation of molten material boundaries in various discharge duration with various R_{pc}

Figure 16 demonstrates a cross-section image for the crater acquired within various dielectrics fluids with varying both polarity and discharge of pulse. Seems that the positive polarity to have melted further material than negative polarity. The depth of molten material, h_{melt}, was much greater for positive polarity, whereas the diameter of molten material, d_{melt}, was much larger with negative polarity. This means that the radius of plasma varied depending on the polarity.

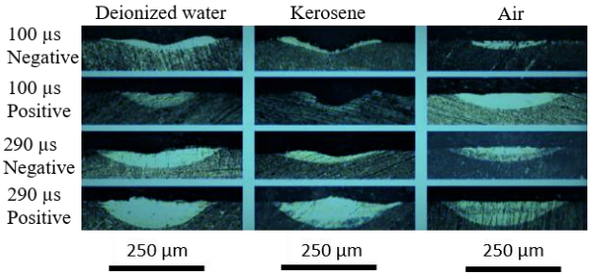

FIGURE 16. Craters cross section obtained in various dielectrics with varying both polarities and pulse discharge

The value of X is specified in Table 2. Regardless of dielectric kind, for positive polarities, X's value was extremely high. The outcome was consistent, according to (Xia, Kunieda & Nishiwaki 1996).

TABLE 2. X values with varying both polarities and pulse discharge in various dielectrics

Parameters (units)		Dielectrics		
Pulse discharge	Polarity	Deionized water (%)	Kerosene (%)	Air (%)
100µs	-ve	38.55	49.05	35.47
100µs	+ve	41.37	51.24	56.08
290µs	-ve	50.16	41.22	48.14
290µs	+ve	54.37	57.08	52.52

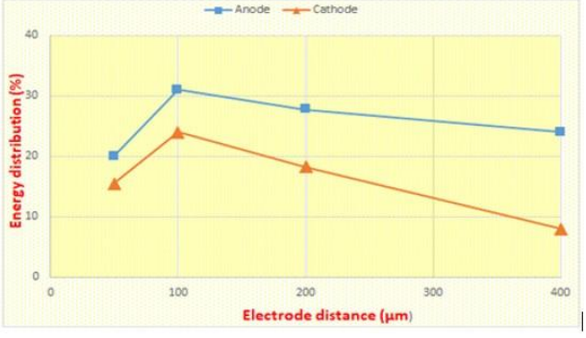

FIGURE 17. Comparison between distributions of energy into the workpiece in various electrode distances of different polarities

EFFECT OF ELECTRODE DISTANCE

Figure 17 demonstrates the influence of electrode distance on the energy distribution. The distribution of energy into an anode is greatly affected by the distance of the gap as can be seen in Figure 17. By increasing the distance of the gap, the distribution of energy into both cathode and anode decreases. This is mostly due to the discharge plasma's radius. (Kojima, Natsu & Kunieda 2008) measured the radius of the plasma channel by the spectroscopic approach and they found that, the radius of the plasma channel increased after increasing the distance of inter-electrode. The implication is that the increment of the distance of inter-electrode will lead to a decrement of the power density applied on the surface of both tool electrode and workpiece. FEM simulation has been done with different value of R_{pc}, and the results show that the value of R_{pc} is a significant factor which affects the shape and area of the melted zone; the area of the melted zone decreases with increasing R_{pc}. In this work, the simulation results show that the R_{pc} increases after increasing distance of interelectrode. As a result, the findings are consistent with those of (Kojima, Natsu & Kunieda 2008), who used a spectroscopic approach to measure the radius of the discharge plasma.

The data in Figure 18 reveals that discharge duration is another significant parameter that can influence the energy distribution characteristics. Regardless of polarity, the amount of energy distribution ratio reduces gradually as the discharge duration increases. The findings are consistent with those obtained by other researchers for hard material machining.

In their work on EDM of tungsten-carbide over a broad spectrum of discharge durations, (H. Singh 2012; H. Singh & Shukla 2012) have also recorded findings of a similar nature. In general, the

ratio of energy distribution should increase as the discharge duration increases, since higher discharge duration will result in more electrode discharge energy being deposited at the surface, melting and evaporating the material quickly. The increasing radius of the discharge plasma at high discharge duration causes this surprising effect. As the radius of the discharge plasma becomes high, the power density decreases, and the absorbed heat energy per unit area by the workpiece is decreased, which thus the characteristics of heat conduction within the electrodes were influencing.

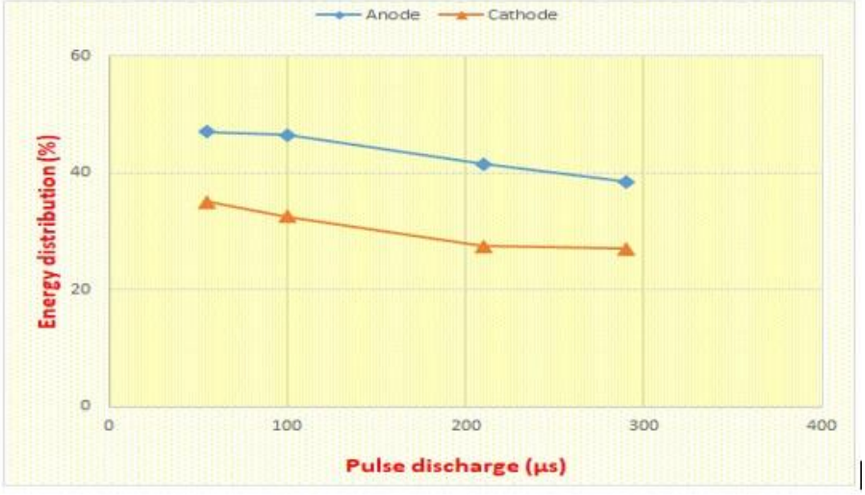

FIGURE 18. Comparison between distributions of energy into the workpiece in various discharge durations of different polarities.

DISCUSSION AND COMPARISON BETWEEN PREVIOUS WORKS AND THE FINDINGS OBTAINED FROM THIS PAPER

The ratio of energy distribution, X, was slightly higher in this study than in previous studies (Van Dijck 1973; Hayakawa et al. 2001; Joshi & Pande 2010b; H. Singh & Shukla 2012; Xia, H., Kunieda, M. & Nishiwaki 1996). According to the findings of (Joshi & Pande 2010b), a thermal physical simulation of a single discharge, they predicted the shape of the crater and MRR; in their study, they considered the magnitude of X was to be 18.3%. They reported that their model was found to predict findings that were similar to the experimental findings. However, we found that in their model, the efficiency of flushing (defined as "efficiency of the removal" in current work) was presumed to be 100%, implying that the molten material was totally removed from the workpiece and that no recast layer was deposited on the machined surface. The supposition was not consistent with the findings of the current experiments of this work, and the findings reported by previous researchers (Van Dijck 1973; Zahiruddin &

Kunieda 2012). The efficiency of removal was less than 10% confirmed experimentally by (Van Dijck 1973). In the current experiment, the highest efficiency for removal was not more than 16%. As seen in Figure 9, the majority of molten material was deposited on the machined surface rather than being removed, particularly when the discharge duration was long. The efficiency of removal for micro and sinking EDM was recently investigated and compared (Zahiruddin & Kunieda 2012). They discovered that micro EDM had a considerably higher efficiency of removal than sinking EDM due to significantly higher heat flux density. Despite this, (Zahiruddin & Kunieda 2012) found that the removal efficiency of micro EDM was less than 20%. (Allen & Chen 2007b), who simulated the residual stress and material removal of micro EDM, considered an X value of 8% in their thermo-numerical model. As the temperature approached and exceeded its melting point, the element was “killed”in their model. This is identical to the assumption that the removal efficiency was 100% (Joshi & Pande 2010b). In a study by (H. Singh & Shukla 2012), who experimentally determined the distribution of energy within the anode, the ratio of energy distribution was stated to be 6-26%. According to (Xia, Kunieda & Nishiwaki 1996), the energy distributed within anode and cathode was approximately 40% and 25%, respectively. Above 90% of the heat, is conducted within the electrodes (Van Dijck 1973).

Based on a magneto-hydrodynamics study of the steady-state arc, (Hayakawa et al. 2001) discovered that almost all of the discharge power is conducted within the electrodes and that heat dissipated by convection and radiation is neglectable. In a study by (Van Dijck 1973; Xia, H., Kunieda, M. & Nishiwaki 1996), the ratio of energy distribution was also determined experimentally. (Xia, Kunieda & Nishiwaki 1996; Van Dijck 1973) found results that were quite similar to those of this research.

The disparity between the relatively low ratio of energy distribution stated by (H. Singh & Shukla 2012) and the relatively high ratio of energy distribution reported by (Van Dijck 1973; Xia, Kunieda & Nishiwaki 1996; Hayakawa et al. 2001) is most likely due to different conditions of an experiment as; the electrode material, working fluid composition, and so on. Furthermore, one of the causes is maybe the error of methodology and measuring equipment.

CONCLUSION

Studying the distribution of energy and diameter of plasma channel during WEDM process has been studied and the work can be concluded as follows:

1. A new approach for determining the ratio of energy distribution into workpiece and radius of plasma channel was proposed by this study.

2. The ratio of distribution of energy and radius of the plasma channel can be determined by measuring the measured and simulated boundaries of the molten material.

3. The expanded of the plasma radius during the discharge was confirmed by this work.

4. According to the findings of this study, the power density was a significant parameter effects on removal of material and energy efficiency.

5. Due to the higher power density, removal of material and energy efficiency were much higher with short pulse durations than with long pulse durations.

6. The study's findings indicate that plasma channel expansion should be considered in order to be further consistent with the real WEDM process.

7. The experiment carried out in deionized water dielectric showed that the influence of polarity was significant.

8. From findings obtained in this study, it can be observed that the ratio of distribution of energy reduces with the increase of distance of inter- electrodes and discharge of pulse due to the expansion of the discharge plasma.

9. By considering the distance of inter-electrode and discharge of pulse, the polarity is another one of significant factor which can highly influence on the characteristics of distribution of energy.

10. It seems that the method proposed in this study is a strong method for investigating of the basic mechanism of WEDM.

11. Value of Xcon obtained with expand plasma radius was much smaller than obtained with constant plasma radius.

ACKNOWLEDGEMENT

The authors gratefully would like to acknowledge the support from the Fundamental Research Grant Scheme (FRGS) under a grant number of FRGS/6/2016/UniMAP/PPPI/9003-00573 from the Ministry of Education Malaysia.

DECLARATION OF COMPETING INTEREST

None

REFERENCES

Abu Q. & Jaber, E. et al. 2019. Advanced electric discharge machining of stainless steels: Assessment of the state of the art, gaps and future prospect. *Materials* 12(6): 907.

Allen, P. & Xiaolin, C. 2007b. Process simulation of micro electro-discharge machining on molybdenum. *Journal of materials processing technology* 186(1–3): 346–55.

Bilal, A., Muhammad, P.J., Didier, T. & Asma, P. 2019. Electro-discharge machining of ceramics: A Review. *Micromachines* 10(1): 10.

Escobar, A.M., Lange, D.de. & Castillo, H.I.M. 2020. Simplified plasma channel formation model for the electrical discharge machining process. *The International Journal of Advanced Manufacturing Technology* 106(1–2): 143–53.

Frans, V.D. 1973. Physico-mathematical analysis of the electro discharge machining process. *Dissertation KU Leuven, The Netherlands*.

Gostimirovic, M. et al. 2018. Inverse electro-thermal analysis of the material removal mechanism in electrical discharge machining. *The International Journal of Advanced Manufacturing Technology* 97(5–8): 1861–71.

Hayakawa, S., Masaaki, Y., Masanori, K. & Nobuhiko, N. 2001. Time variation and mechanism of determining power distribution in electrodes during EDM process. *International journal of electrical machining* 6: 19–25.

Hou, P. et al. 2014. Influence of open-circuit voltage on high-speed wire electrical discharge machining of insulating zirconia. *International Journal of Advanced Manufacturing Technology*.

Izquierdo, B. et al. 2009. A numerical model of the EDM process considering the effect of multiple discharges. *International Journal of Machine Tools and Manufacture* 49(3–4): 220–29.

Joshi, S.N. & Pande, S.S. 2010b. Thermo-physical modeling of die-sinking EDM Process." *Journal of Manufacturing Processes* 12(1): 45–56.

Kitamura, T. & Masanori, K. 2014. Clarification of EDM gap phenomena using transparent electrodes. *CIRP Annals - Manufacturing Technology*.

Kojima, A., Natsu, W. & Kunieda, M. 2008. Spectroscopic measurement of arc plasma diameter in EDM. *CIRP Annals.- Manufacturing Technology* 57(1): 203–7.

Kumar, P., Manowar, H., Purushottam, K.S. & Alok, K.D. 2015. A new method for modeling of cathode and anode erosion in micro-EDM process. *Int J Appl Eng Res* 10: 24.

Liu, J.F. & Guo, Y B. 2016. Thermal modeling of EDM with progression of massive random electrical discharges. *Procedia Manufacturing*.

Rajendran, R. & Vendan, S.P. 2015. Single discharge finite element simulation of EDM process. *Journal of Advanced Manufacturing Systems* 14(02): 75–89.

Revaz, B., Witz, G. & Flükiger, R. 2005. Properties of the plasma channel in liquid discharges inferred from cathode local temperature measurements. *Journal of Applied Physics* 98(11): 1–7.

Saleh Warregh Adel & Mohd Zahiruddin, Md.Z. 2018. Experimental investigation of workpiece deformation due to WEDM. *MS&E* 429(1): 12011.

Shabgard, M., Soleyman, S. and Mirsadegh, S. 2016. Novel approach towards finite element analysis of residual stresses in electrical discharge machining process. *The International Journal of Advanced Manufacturing Technology* 82(9–12): 1805–14.

Shahri, H.R.F., Ramezanali, M., Mehdi, A. & Amir, A. 2017. A comparative investigation on temperature distribution in electric discharge machining process through analytical, numerical and experimental methods. *International Journal of Machine Tools and Manufacture* 114: 35–53.

Shao, B. & Kamlakar, P.R. 2015. Modelling of the crater formation in micro-EDM. *Procedia CIRP* 33: 376–81.

Shen, Y. et al. 2014. Determining the energy distribution during electric discharge machining of Ti–6Al–4V. *The International Journal of Advanced Manufacturing Technology* 70(1–4): 11–17.

Singh, H. 2012. Experimental study of distribution of energy during EDM process for utilization in thermal models." *International Journal of Heat and Mass Transfer*.

Singh, H. & Shukla, D.K. 2012. Optimizing electric discharge machining parameters for tungsten-carbide utilizing thermo-mathematical modelling. *International Journal of Thermal Sciences* 59: 161–75.

Singh, M., Prakhar, S., Ramkumar, J. & Rao, R.V. 2020. Multi-spark numerical simulation of the micro-EDM process: An extension of a single-spark numerical study. *The International Journal of Advanced Manufacturing Technology* 1–15.

Xia, H., Kunieda, M. & Nishiwaki, N. 1996. Removal amount difference between anode and cathode in EDM process. *International Journal of Electrical Machining*.

Xia, H., Masanori, K. & Nobuhiko, N. 1996. Removal amount difference between anode and cathode in EDM process. *Ijem* 1: 45–52.

Xue, R., Lin, G., Kai, Y. & Fawang, Z. 2012. Energy distribution and material erosion model in near-dry electrical discharge milling. *Jixie Gongcheng Xuebao(Chinese Journal of Mechanical Engineering)* 48(21): 175–82.

Zahiruddin, M. & Masanori, K. 2010. Energy distribution ratio into micro EDM electrodes. *Journal of Advanced Mechanical Design, Systems, and Manufacturing* 4(6): 1095–1106.

Zahiruddin, M. & Masanori, K. 2012. Comparison of energy and removal efficiencies between micro and macro EDM. *CIRP Annals - Manufacturing Technology*.

Zahiruddin, M. & Masanori, K. 2016. Analysis of micro fin deformation due to micro EDM. *Procedia CIRP*.

Zhang, M. et al. 2016. Comparisons of single pulse discharge crater geometries in EDM and EAM. *Journal of Manufacturing Processes* 22: 74–81.